Proc. NIPR Symp. Antarct. Geosci., **9**, 76–90, 1996

SUBVOLCANIC ZONED GRANITIC PLUTON IN THE BARTON AND WEAVER PENINSULAS, KING GEORGE ISLAND, ANTARCTICA

Jong Ik LEE[1], Jeong HWANG[1], Hyeoncheol KIM[1], Cheon Yun KANG[1], Mi Jung LEE[2] and Keisuke NAGAO[3]

[1]*Polar Research Center, Korea Ocean Research & Development Institute, Ansan, P.O. Box 29, Seoul, 425-600, Korea*
[2]*Department of Earth Sciences, Seoul National University, 151-742, Seoul, Korea*
[3]*Institute for Study of the Earth's Interior, Okayama University, Misasa, Tottori 682-01*

Abstract: The subvolcanic granitic pluton in the Barton and Weaver Peninsulas, King George Island, is mainly composed of granodiorite with small volumes of gabbro, diorite and aplitic dikes. The pluton shows a vertically compositional zonation; the lower part consists of gabbro and diorite, whereas the upper part is mainly granodiorite. Various geochemical signatures of the pluton confirm that all subunits of the pluton were formed by accumulation and fractionation in a calc-alkaline magma at a shallow level of the crust. The positive Sr and Eu anomalies as well as textural features of gabbro strongly support that gabbro was the cumulate derived from accumulation of calcic plagioclase and *in situ* crystallization of ferromagnesian minerals. Taking into account the geochemical features of gabbro as a cumulate, the primary magma of the pluton is considered to have been intermediate (dioritic or quartz dioritic) in composition.

key words: subvolcanic zoned pluton, King George Island, accumulation, primary granitic magma

1. Introduction

The South Shetland Islands (SSI) are a calc-alkaline island arc formed on a crustal block, separated from the Antarctic Peninsula by the young marginal basin named Bransfield Strait. The crustal thickness of SSI is about 30 km and increases toward the northern Antarctic Peninsula (GUTERCH *et al.*, 1990). The age of plutonic activity in SSI ranges from 120 to 10 Ma (BIRKENMAJER *et al.*, 1986). Recent radiogenic age determinations reveal the apparently lateral northeastward migration of plutonic activity from the late Cretaceous to the Miocene. Though the reason for this migration is considered to be related to the relative plate motion around the Pacific margin of the northern Antarctic Peninsula, the exact reason is still controversial.

The subvolcanic Eocene granitic pluton in the Barton and Weaver Peninsulas, King George Island, formerly described as "quartz diorite" (BARTON, 1964), is mainly composed of granodiorite with small volumes of gabbro, diorite and aplitic dikes. The

lower part of the pluton consists of gabbro and diorite, whereas the upper part is mainly granodiorite. So the pluton shows a vertically compositional zonation (Lee *et al.*, 1994). Various geochemical signatures of the pluton and associated volcanic equivalents in the Barton and Weaver Peninsulas show a calc-alkaline nature in a volcanic arc setting (Smellie *et al.*, 1984; Birkenmajer *et al.*, 1991).

In this paper, we will describe the petrological and geochemical characteristics of the subvolcanic pluton in the Barton and Weaver Peninsulas, and discuss the origin of vertical zonation of the pluton and the primary magma composition.

2. Geological Setting

King George Island, situated in the middle of the South Shetland Islands, consists of several tectonic blocks bounded by longitudinal faults (Fig. 1). The downthrown Fildes and Warszawa/Krakow blocks are located in the north and south of the island, respectively. The upthrown Barton horst makes up the axial part of the island. The stratigraphic sequence of King George Island includes upper Cretaceous to lower Miocene, mostly calc-alkaline, predominantly subaerial volcanic and volcanoclastic rocks, intruded by moderate-sized granitic plutons. The considerable differences in stratigraphic succession and lithologies among the blocks suggest large-scale lateral displacement of the blocks along the Ezcurra and Collins strike-slip faults (Birkenmajer, 1983).

The Barton and Weaver Peninsulas belong to the Barton horst. The southern Barton and Weaver Peninsulas are composed of a volcanoclastic succession of mainly intermediate composition (Fig. 2). Along the southern coast, poorly-sorted agglomerate, tuffaceous sandstone, purple or pale green sandstone and later intrusive andesite occupy the lower unit of volcanoclastic succession. Lots of plant fossils indicating late Paleocene to Eocene in age and tropical to subtropical environment occur in the purple sandstone or siltstone layers (Chun *et al.*, 1994). The upper unit of the southern peninsula consists dominantly of andesitic tuff and lava.

The northern Barton Peninsula, separated from the southern peninsula by NW-SE trending fault, comprises andesitic tuff, basaltic andesite and a granitic pluton (Fig. 2). Basaltic andesite, which has usually undergone propylitic to advanced argillic alteration, is widely developed in the northern peninsula (Hwang *et al.*, 1996). The granitic pluton, having intruded into basaltic andesite on the north and bounded by andesitic tuff and lava on the south, is mainly composed of granodiorite with minor gabbro, diorite and aplitic dikes. The lower part of the pluton comprises mafic facies (gabbro and diorite), whereas the upper part mainly occupies granodiorite. Hence the pluton is likely to be a vertically zoned pluton.

Two K-Ar biotite ages of granodiorite determined by the present authors are 41.9±0.9 Ma and 41.2±0.9 Ma, respectively (Table 1). Park (1989) reported similar whole-rock K-Ar ages (42 to 45 Ma) from granodiorite in the Barton Peninsula. Combined with previous results (Watts, 1982; Pankhurst and Smellie, 1983; Kang and Jin, 1989; Park, 1989), the pluton is thought to have been intruded in the Eocene.

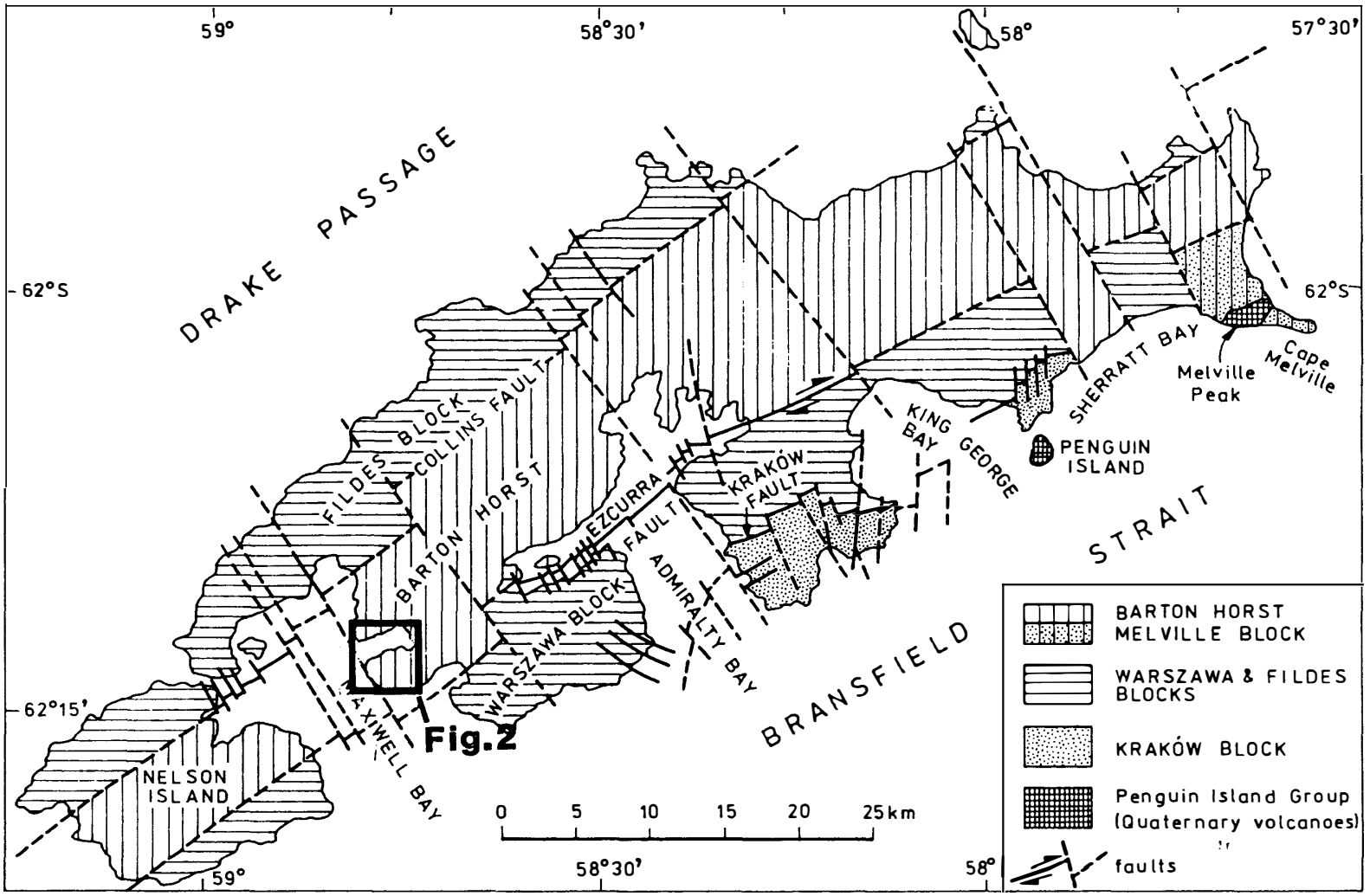

Fig. 1. Main tectonic units of King George Island (after BIRKENMAJER, *1983).*

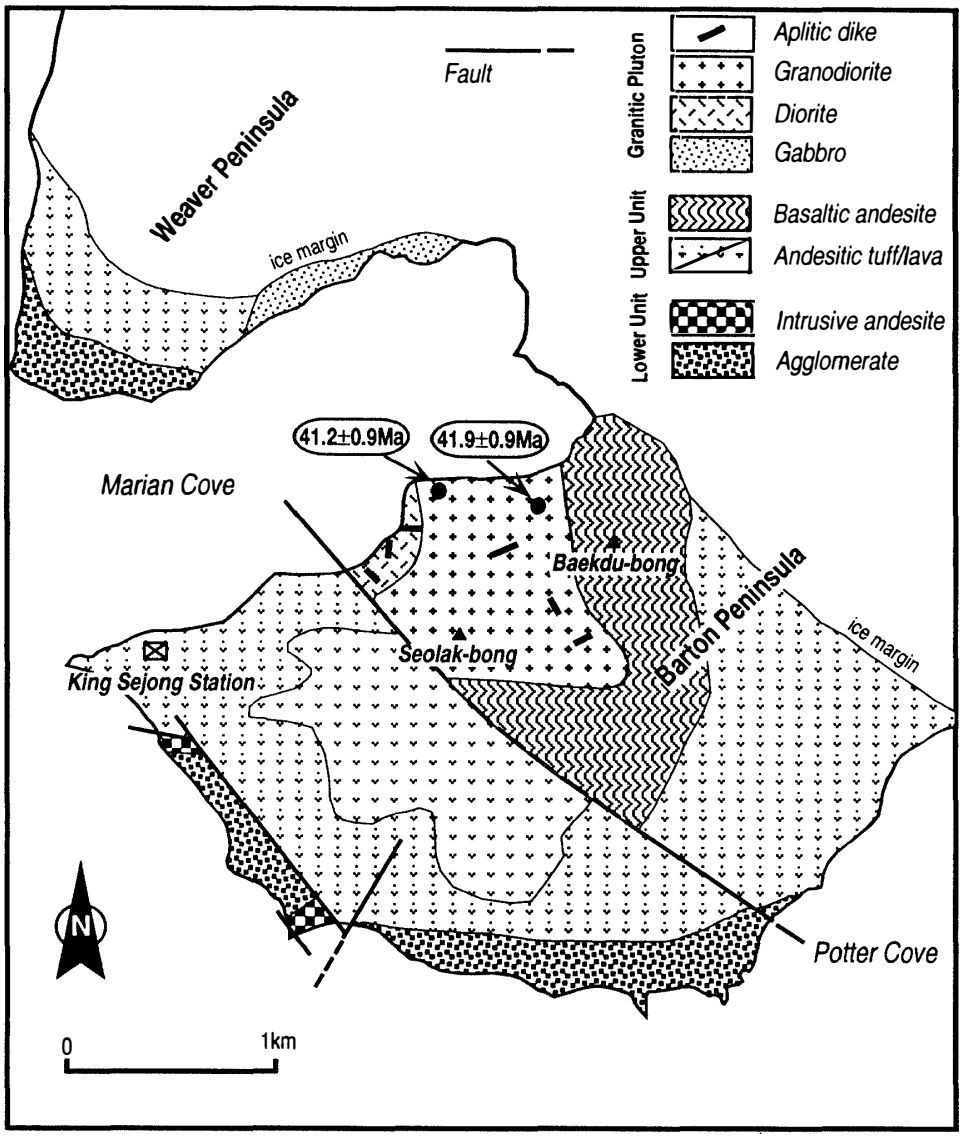

Fig. 2. Geological map of the Barton and Weaver Peninsulas, King George Island. Location and K-Ar biotite ages of granodiorite determined by the authors are shown.

Table 1. Analytical results of K-Ar biotite ages from the granitic rocks.

Rock type	Sample No.	Mineral	K* (wt%)	[^{40}Ar]rad** (E^{-8}cc/g)	Atm.^{40}Ar (%)	Age** (Ma)
Granodiorite	93011506	biotite	6.77	1096±11	4.26	41.2±0.9
Granodiorite	93122508	biotite	7.03	1158±11	4.63	41.9±0.9

* K concentration of biotites was determined by atomic absorption method at KORDI, and maximum error of it was estimated to be ±2%.

** Calculation of argon isotopic ratio and age was followed by the procedure of NAGAO *et al.* (1996).

3. Petrography of the Pluton

Average modal compositions of the granitic rocks are listed in Table 2. A triangular diagram of modal quartz, plagioclase and alkali feldspar illustrates that the pluton has wide compositional range from gabbro to granite, but is mainly composed of granodiorite (Fig. 3). An interesting feature is the compositional gaps between subunits. For example, the rock having quartz dioritic composition is completely absent in the diagram. Though sharp boundaries among subunits could not be identified in the field because of poor outcrops, the pluton is likely to be a vertically zoned pluton. Mafic facies (gabbro and diorite) are only distributed around the coast, whereas the main body of granodiorite comprises a high mountainous area around Seolak-bong (Fig. 2).

Dark greenish, medium-grained gabbro in the Weaver Peninsula is characterized by cumulate textures with mafic minerals occupying the interstices between euhedral to subhedral plagioclase grains (Fig. 4A). Mafic minerals include olivine, orthopyroxene, clinopyroxene and Fe-Ti oxides with minor hornblende and biotite. The most abundant euhedral to subhedral plagioclase having normal zoning, is considered to be a cumulus phase. Anhedral clinopyroxene, the second most abundant phase, frequently encloses cumulus plagioclase. This clinopyroxene is interpreted to have been formed by *in situ* crystallization from intercumulus liquid.

Fine-grained diorite distributed along the southern coast of Marian Cove consists of plagioclase, quartz, pyroxene, hornblende, biotite and Fe-Ti oxides with minor apatite (Fig. 4B). Chlorite and epidote are the common secondary minerals. Compared with gabbro, diorite contains more hornblende and biotite, but less pyroxene. Most of the mafic phases occur as aggregates with each other in the grain

Table 2. Average modal compositions of the granitic rocks.

Rock type	Gabbro	Diorite	Granodiorite	Aplitic dike
No. of mea.*	3	4	18	3
Af			15.8	51.4
Pl	64.7	69.7	49.0	12.7
Qz	0.4	2.3	18.2	28.6
Px	23.4	2.8	1.2	1.7
Hb	2.7	5.3	6.7	1.6
Bt	0.1	10.1	4.4	0.9
Zir				0.1
Apt		0.3		
Chl	2.5	2.7	1.0	0.2
Cc	0.1			0.1
Epi	0.1	0.7	0.2	0.1
Opq	6.1	6.3	3.5	2.6

*Number of measurements.

Abbreviations: Af=alkali feldspar, Pl=plagioclase, Qz=quartz, Px=pyroxene, Hb=hornblende, Bt=biotite, Zir=zircon, Apt=apatite, Chl=chlorite, Cc=calcite, Epi=epidote, Opq=opaque minerals.

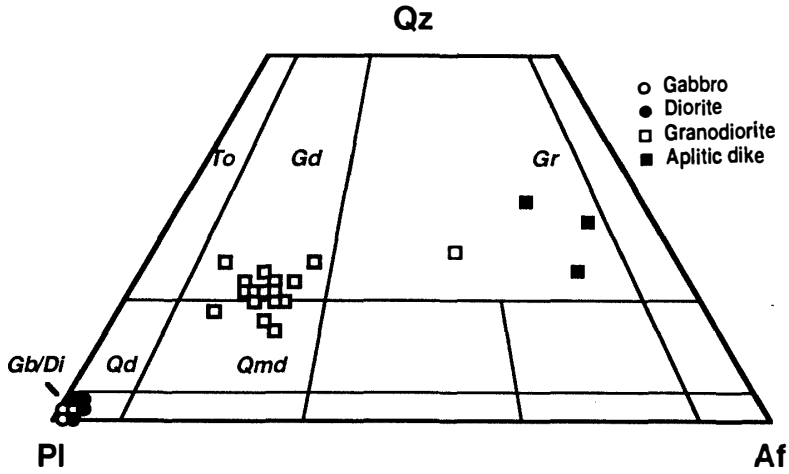

Fig. 3. Triangular diagram of modal quartz, plagioclase and alkali feldspar. The classification of plutonic rocks was followed by recommendation of IUGS (1973) subcommission. Abbreviations: Qz=quartz, Pl=plagioclase, Af=alkali feldspar, Gb=gabbro, Di=diorite, Qd=quartz diorite. Qmd=quartz monzodiorite, To=tonalite, Gd=granodiorite, Gr=granite.

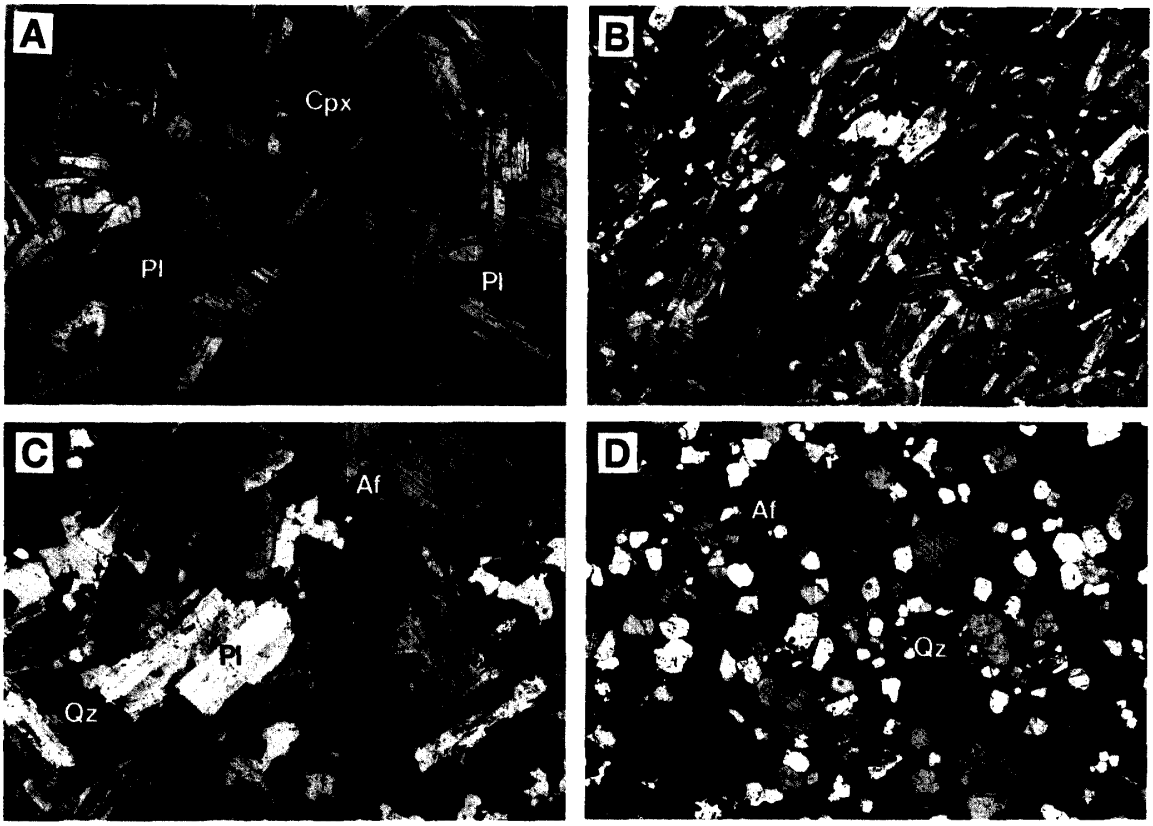

Fig. 4. Photomicrographs of the granitic rocks in the Barton and Weaver Peninsulas. A: gabbro, B: diorite, C: granodiorite: D; aplitic dike. Gabbro (A) is characterized by cumulus texture with anhedral clinopyroxene occupying the interstices between euhedral plagioclases. All photomicrographs were taken under cross polars. The full widths of all photomicrographs are about 5 mm. Abbreviations: Cpx=clinopyroxene, Pl=plagioclase, Af=alkali feldspar, Qz=quartz.

boundaries of plagioclase.

Medium-grained granodiorite is composed of plagioclase, quartz, alkali feldspar, hornblende, biotite and Fe-Ti oxides (Fig. 4C). Minor phases are pyroxene, zircon and apatite. Chlorite, epidote and rare calcite occur as alteration products. Sulfide minerals such as chalcopyrite, pyrite and bornite are closely associated with alteration minerals (Hwang *et al.*, 1996). Hornblende and biotite with variable quantity from sample to sample are mostly aggregated with magnetite. Frequently observed miarolitic cavities and micrographic intergrowths between alkali feldspar and quartz support that the magma was saturated with vapor near its solidus and decompressed to a certain degree.

Equigranular and very fine-grained aplitic dikes with a few centimeters in thickness intruded into diorite and granodiorite. They are composed of alkali feldspar, quartz and plagioclase with subordinate hornblende, biotite, zircon and Fe-Ti oxides (Fig. 4D). Abundant miarolitic cavities contain secondary quartz, alkali feldspar and epidote. Micrographic textures are also observed in some sections.

4. Geochemistry

Whole rock analysis of major elements was carried out using an XRF (Philips model PW1480) at the Polar Research Center, Korea Ocean Research & Development Institute (KORDI), following the procedure outlined by Lee (1994). Trace and rare earth elements were analyzed by an ICP-MS (VG PQ II plus model) at Korea Basic Science Institute.

The analytical results are given in Table 3. Oxide variation diagrams (Fig. 5) show good fractionation trends of ferromagnesian minerals and plagioclase. TiO_2, Al_2O_3, FeO* (total Fe), MgO and CaO contents progressively decrease with increasing SiO_2 content. Na_2O and P_2O_5 contents increase from gabbro to diorite, and then decrease toward more felsic facies, which suggests that the fractionation of sodic plagioclase and apatite started from granodioritic composition. Continuous increase of K_2O content means that K-bearing minerals such as alkali feldspar and/or biotite could not be fractionated. Note that oxide variation diagrams also show compositional gaps between subunits as shown in the triangular diagram of modal composition. The AFM diagram (Fig. 6) shows the differentiation trend of the calc-alkaline series; there was no iron enrichment during differentiation. Molar $Al_2O_3/(Na_2O+K_2O+CaO)$ ratios continuously increase as SiO_2 content increases and all of the subunits have metaluminous and I-type granitoid geochemical nature (Fig. 7).

Trace element variation diagrams (Fig. 8) also illustrate good fractionation trends except for the trends of chalcophile elements (Cu, Pb and Zn). Incompatible elements (Rb, Ba and Th) (Fig. 8) and LILE/HFSE ratios (Fig. 9) continuously increase toward more fractionated facies. In the spider diagrams (Fig. 9) normalized to a primordial mantle composition (Wood *et al.*, 1979), Nb negative anomalies which are typically observed in subduction-related magmatism (McCulloch and Gamble, 1991) can be seen in diorite, granodiorite and aplitic dikes. Gabbro shows a strong Sr positive anomaly. LREE/HREE ratios progressively increase toward more fraction-

Table 3. Analytical results of major, trace and rare earth elements of the granitic rocks.

Rock type	Gb	Gb	Gb	Di	Di	Di	Di	Gd	Gd
Sample No.	9401 0801	9401 0802	9401 0803	9212 2901	9301 0901	9301 1504	9312 2601	9212 2902	9212 2903
				Major oxides (wt%)					
SiO_2	46.89	46.11	47.04	54.12	51.93	55.18	52.99	64.74	69.74
TiO_2	0.58	0.74	0.86	0.69	0.71	0.77	0.69	0.38	0.28
Al_2O_3	19.42	21.75	18.79	17.91	17.79	17.77	17.69	15.25	13.60
FeO*	9.06	8.53	9.74	7.31	7.68	7.45	8.04	4.03	3.08
MnO	0.16	0.12	0.15	0.16	0.16	0.14	0.16	0.09	0.07
MgO	6.92	4.32	6.21	4.30	3.96	3.53	4.39	1.59	1.21
CaO	11.30	13.19	12.05	7.99	8.79	7.55	7.68	3.95	2.39
Na_2O	2.15	2.32	2.52	3.85	3.63	3.89	3.76	3.94	3.21
K_2O	0.12	0.26	0.17	0.98	0.91	1.26	0.92	3.19	5.02
P_2O_5	0.03	0.05	0.08	0.22	0.20	0.24	0.18	0.14	0.07
H_2O^-	1.52	1.21	1.35	0.95	1.74	0.98	1.42	0.85	0.56
H_2O^+	0.97	0.75	0.55	0.86	1.35	0.87	1.25	1.35	0.85
Total	99.11	99.34	99.52	99.34	98.84	99.62	99.17	99.50	100.07
				Trace elements (ppm)					
Rb	3.1	4.8	5.0	22.2	21.1	27.1	22.9	88.3	98.2
Ba	54.9	92.3	87.2	201.5	210.5	230.3	199.6	404.3	445.5
Th	0.3	0.3	0.4	2.7	2.5	2.2	2.2	8.2	9.2
Nb	4.2	3.3	3.7	6.7	5.2	5.6	5.7	6.9	6.9
Sr	827.7	788.9	797.2	517.7	575.8	561.9	651.0	339.8	191.7
Y	7.9	9.8	9.2	18.1	17.1	22.7	21.0	20.6	18.9
Pb	1.9	3.4	3.4	10.6	10.7	12.8	9.7	11.7	9.4
Co	80.2	58.2	59.9	29.3	51.0	37.8	45.8	14.7	9.1
Cu	60.1	120.3	127.4	101.5	134.8	343.1	523.5	182.4	272.6
Zn	125.5	115.9	119.2	142.8	113.8	147.9	212.2	70.7	66.6
				Rare earth elements (ppm)					
La	2.4	3.3	3.3	10.0	12.8	12.3	10.7	18.0	14.1
Ce	5.2	7.2	7.0	23.0	27.5	28.0	23.9	41.1	30.8
Nd	3.7	4.9	3.4	14.0	16.0	15.6	12.9	21.5	15.6
Sm	1.2	1.1	1.2	3.3	3.6	3.2	2.9	3.9	3.4
Eu	0.6	0.7	0.6	1.2	1.2	1.3	1.0	1.1	0.7
Gd	1.4	1.6	1.5	3.9	3.9	4.1	3.7	4.8	3.8
Dy	1.0	1.2	1.2	3.3	2.7	3.5	2.7	3.6	3.2
Er	0.6	0.7	0.6	1.8	1.3	1.8	1.6	1.6	1.9
Yb	0.5	0.6	0.5	1.5	1.2	1.5	1.3	1.9	1.8

Abbreviations: Gb=gabbro, Di=diorite, Gd=granodiorite, Ad=aplitic dikes.

ated facies (Fig. 10). Gabbro has positive Eu anomalies, whereas granodiorite and aplitic dikes have negative anomalies. Positive Sr and Eu anomalies of gabbro are considered to be due to accumulation of plagioclase. Low concentrations of Nb and Y (Fig. 11A) and relatively low concentration of Rb (Fig. 11B) compared to typical syn-collision granites in all subunits demonstrate that the pluton was formed under a volcanic arc environment (PEARCE *et al.*, 1984).

Table 3. (Continued)

Rock type	Gd	Gd	Gd	Gd	Gd	Gd	Gd	Gd	Gd
Sample	9212	9212	9212	9301	9301	9301	9301	9301	9301
No.	3003	3004	3005	0302	0303	0308	0902	0904	0905-1
				Major oxides (wt%)					
SiO_2	62.02	61.44	60.37	61.36	60.44	63.18	59.40	62.09	63.08
TiO_2	0.55	0.61	0.60	0.63	0.60	0.48	0.62	0.56	0.56
Al_2O_3	16.06	16.29	16.40	16.23	16.64	15.83	16.80	16.07	15.96
FeO*	5.31	5.49	5.49	5.71	5.64	4.80	5.85	5.38	4.87
MnO	0.13	0.11	0.15	0.12	0.09	0.10	0.11	0.10	0.11
MgO	2.45	2.41	2.77	2.67	2.76	2.14	2.85	2.40	2.17
CaO	5.10	5.03	5.19	5.14	5.36	4.61	5.83	4.58	4.87
Na_2O	3.88	4.08	4.56	3.97	3.99	3.83	4.20	4.04	3.87
K_2O	2.58	2.38	2.37	2.44	2.33	2.76	2.10	2.64	2.75
P_2O_5	0.15	0.18	0.20	0.19	0.16	0.16	0.19	0.16	0.16
H_2O^-	0.45	0.65	0.72	0.87	0.82	0.76	0.84	0.59	0.76
H_2O^+	0.76	0.75	0.57	0.76	0.58	0.88	0.69	0.73	0.49
Total	99.42	99.42	99.39	100.09	99.42	99.53	99.48	99.34	99.63
				Trace elements (ppm)					
Rb	71.8	60.6	51.8	66.8	54.6	82.3	68.0	69.2	72.1
Ba	345.7	334.2	350.3	333.9	281.4	378.5	268.2	347.4	346.6
Th	7.0	6.6	6.0	6.3	5.2	7.4	5.4	7.2	9.0
Nb	6.1	5.5	6.0	6.4	5.7	3.4	5.2	6.3	21.2
Sr	383.9	403.1	406.1	387.4	388.5	374.9	426.7	392.5	337.0
Y	22.9	22.2	22.5	23.2	18.8	24.5	20.8	22.5	22.9
Pb	14.7	11.8	22.8	10.0	6.3	9.7	23.9	6.3	10.1
Co	19.0	20.0	20.8	21.2	19.4	17.9	22.7	17.3	21.3
Cu	134.5	176.4	145.7	113.2	101.8	118.6	161.4	123.3	116.1
Zn	87.3	106.7	97.8	74.7	61.2	78.5	138.2	42.0	100.8
				Rare earth elements (ppm)					
La	16.4	16.8	15.4	16.8	12.9	19.0	14.6	17.0	17.5
Ce	37.2	38.3	36.1	37.6	28.7	42.0	33.0	37.6	39.4
Nd	19.5	21.2	20.3	21.2	16.1	22.1	18.6	20.8	20.0
Sm	4.1	4.5	4.4	4.6	3.5	4.6	3.6	3.9	4.1
Eu	1.2	1.0	1.2	1.1	1.0	1.2	1.1	1.3	1.0
Gd	4.7	4.4	4.4	5.0	4.4	5.1	4.6	5.0	4.4
Dy	3.7	3.8	3.6	3.9	3.2	4.1	3.6	4.0	4.2
Er	2.0	1.8	2.0	2.3	1.7	2.2	2.3	2.2	2.1
Yb	2.1	1.8	1.7	2.0	1.9	2.1	1.7	1.8	2.1

5. Discussion

As mentioned in the above chapter, the petrological and geochemical properties of the granitic pluton in this study suggest that all of the subunits were formed by accumulation and fractionation processes. The positive Sr and Eu anomalies, textural features of gabbro as well as compositional gaps between subunits strongly support that gabbro was the cumulate derived from accumulation of calcic plagioclase near

Table 3. (Continued)

Rock type	Gd	Gd	Gd	Gd	Gd	Gd	Ad	Ad
Sample	9301	9301	9301	9301	9312	9312	9301	9301
No.	0907	1506	1507	1508	2602	2604	0905-2	1503
				Major oxides (wt%)				
SiO_2	61.78	62.49	64.93	64.91	59.33	61.25	68.88	69.84
TiO_2	0.56	0.51	0.38	0.47	0.60	0.49	0.31	0.33
Al_2O_3	16.11	15.97	15.12	15.51	15.94	16.31	14.82	13.11
FeO*	5.41	4.84	4.01	4.26	5.79	5.13	3.02	2.98
MnO	0.12	0.11	0.10	0.10	0.12	0.10	0.08	0.10
MgO	2.56	2.49	1.71	1.87	2.73	2.27	0.21	1.03
CaO	4.99	4.87	3.69	3.96	5.21	4.87	0.89	2.30
Na_2O	4.14	3.92	3.79	3.83	4.14	4.05	3.32	3.47
K_2O	2.45	2.80	3.32	3.17	2.52	2.41	7.45	5.22
P_2O_5	0.18	0.15	0.12	0.13	0.18	0.17	0.04	0.08
H_2O^-	0.68	0.72	0.99	0.81	0.99	0.94	0.32	0.45
H_2O^+	0.69	0.81	1.22	0.75	1.25	1.31	0.25	0.44
Total	99.67	99.67	99.38	99.76	98.79	99.29	99.58	99.36
				Trace elements (ppm)				
Rb	72.9	77.8	97.9	91.1	90.6	77.2	158.6	138.9
Ba	337.9	339.5	397.1	388.1	336.7	348.1	897.9	460.2
Th	6.4	6.5	9.4	10.8	6.6	5.9	11.3	10.9
Nb	70	7.7	8.3	8.1	7.2	6.8	9.9	5.5
Sr	400.8	455.7	427.5	410.2	477.7	503.4	199.9	278.7
Y	25.8	28.6	27.8	31.5	29.5	26.7	23.4	17.5
Pb	9.8	7.5	10.5	7.7	25.4	10.2	50.1	12.0
Co	25.8	26.2	19.7	20.3	29.6	26.8	3.4	14.5
Cu	135.0	136.5	124.0	429.4	221.5	168.9	166.5	137.0
Zn	110.7	96.1	98.5	76.5	115.8	124.3	83.1	115.5
				Rare earth elements (ppm)				
La	18.2	18.0	20.6	20.1	18.2	16.5	37.9	18.5
Ce	40.4	40.7	44.7	47.2	40.5	38.9	78.2	36.5
Nd	19.4	19.8	21.1	22.0	20.1	18.7	34.7	15.5
Sm	4.1	4.0	4.3	4.6	4.5	3.5	6.9	2.6
Eu	1.1	0.9	1.0	1.1	1.0	1.0	1.5	0.8
Gd	4.5	4.7	4.8	5.1	4.9	4.6	6.2	2.9
Dy	4.3	3.9	3.5	3.9	4.0	3.3	4.4	2.4
Er	2.5	2.3	2.1	2.3	2.5	1.9	2.1	1.4
Yb	2.3	1.9	1.9	2.3	2.0	1.8	1.9	1.2

the cooling margins of a crystallizing magma. The subsequent fractionation of ferromagnesian minerals, calcic or sodic plagioclase and Fe-Ti oxides would lead to the formation of more felsic subunits.

In order to sink calcic plagioclase into a magma chamber, plagioclase must be liquidus phase and more dense than primary magma. Calcic plagioclase (An_{90-60}) may sink even in a mafic magma under lower crust in the presence of 3 wt% H_2O (KUSHIRO, 1989). KUSHIRO also observed that the density of a magma would be smaller at lower pressure. The density of calc-alkaline, intermediate magma is much

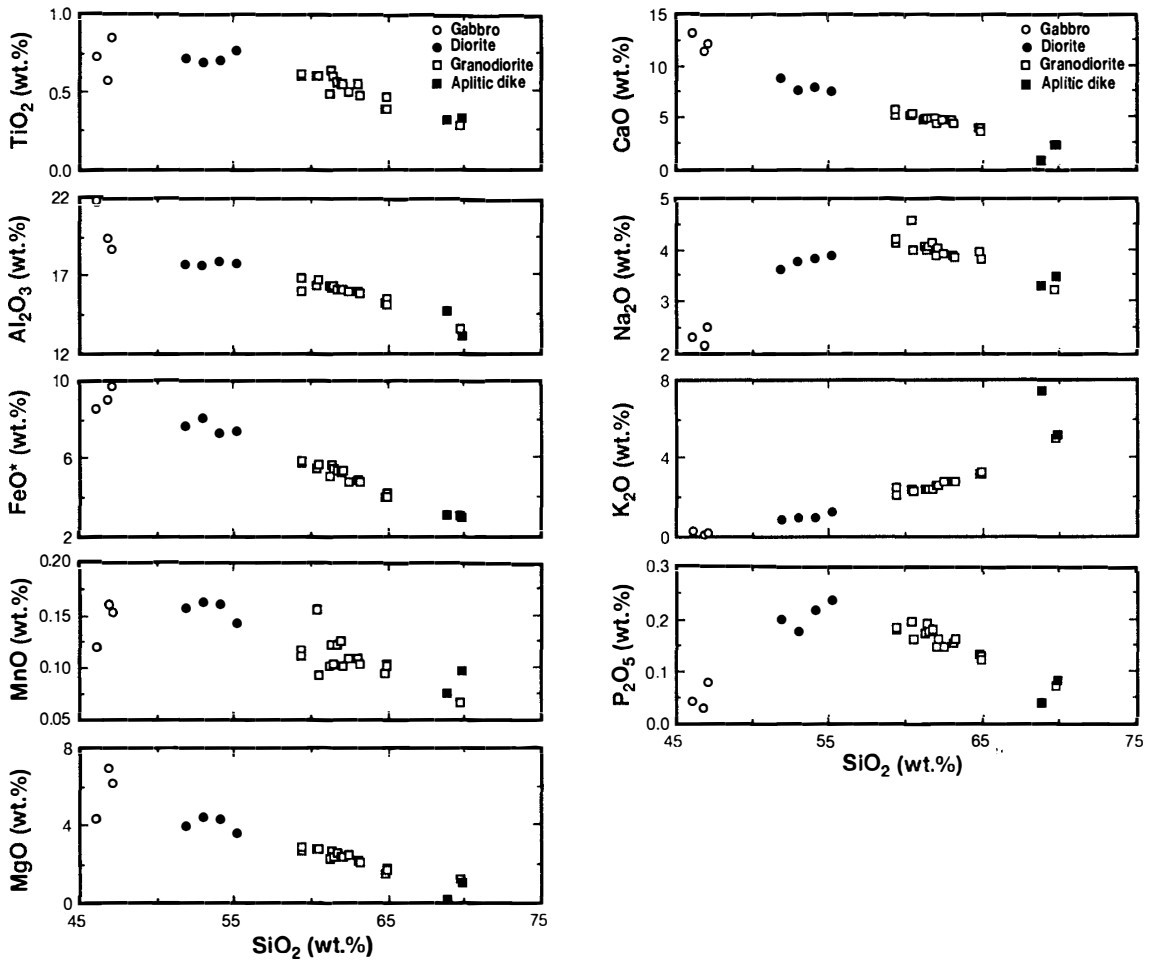

Fig. 5. Oxide variation diagrams of the granitic rocks.

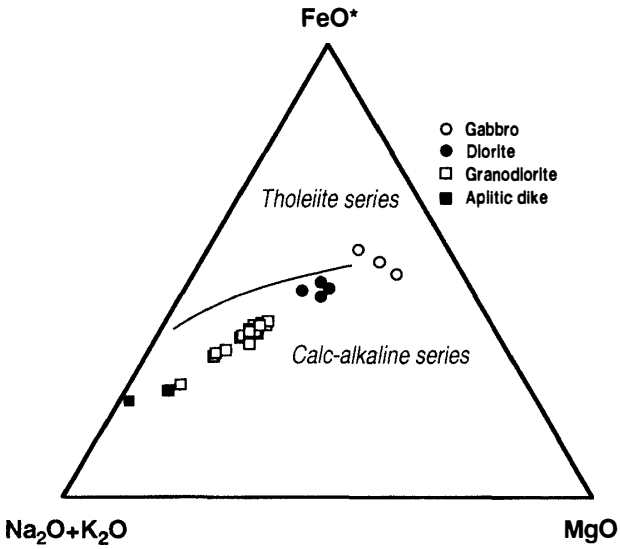

Fig. 6. AFM diagram of the granitic rocks. The boundary curve between tholeiite and calc-alkaline series is from KUNO *(1968).*

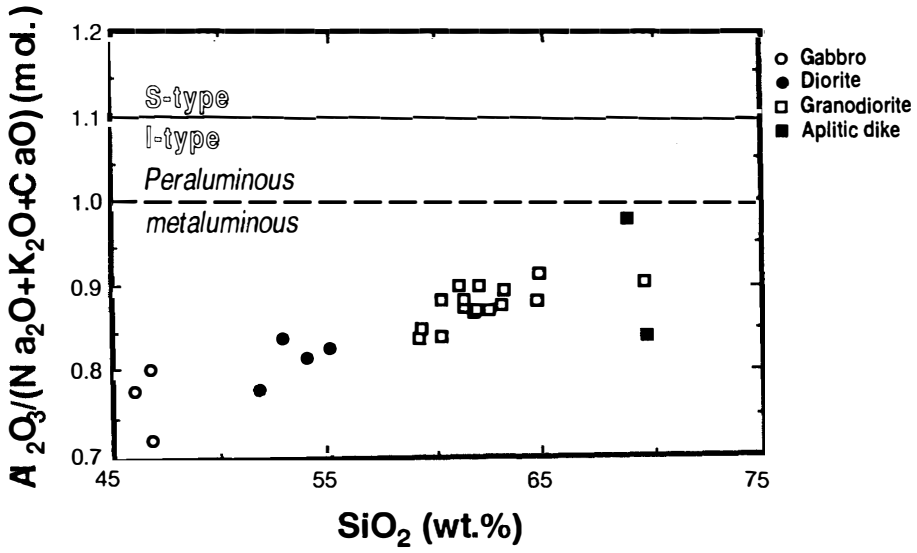

Fig. 7. Molar $Al_2O_3/(Na_2O+K_2O+CaO)$ versus SiO_2 variation diagram. The I-/S-type granitoid boundary is based on HINE *et al. (1978).*

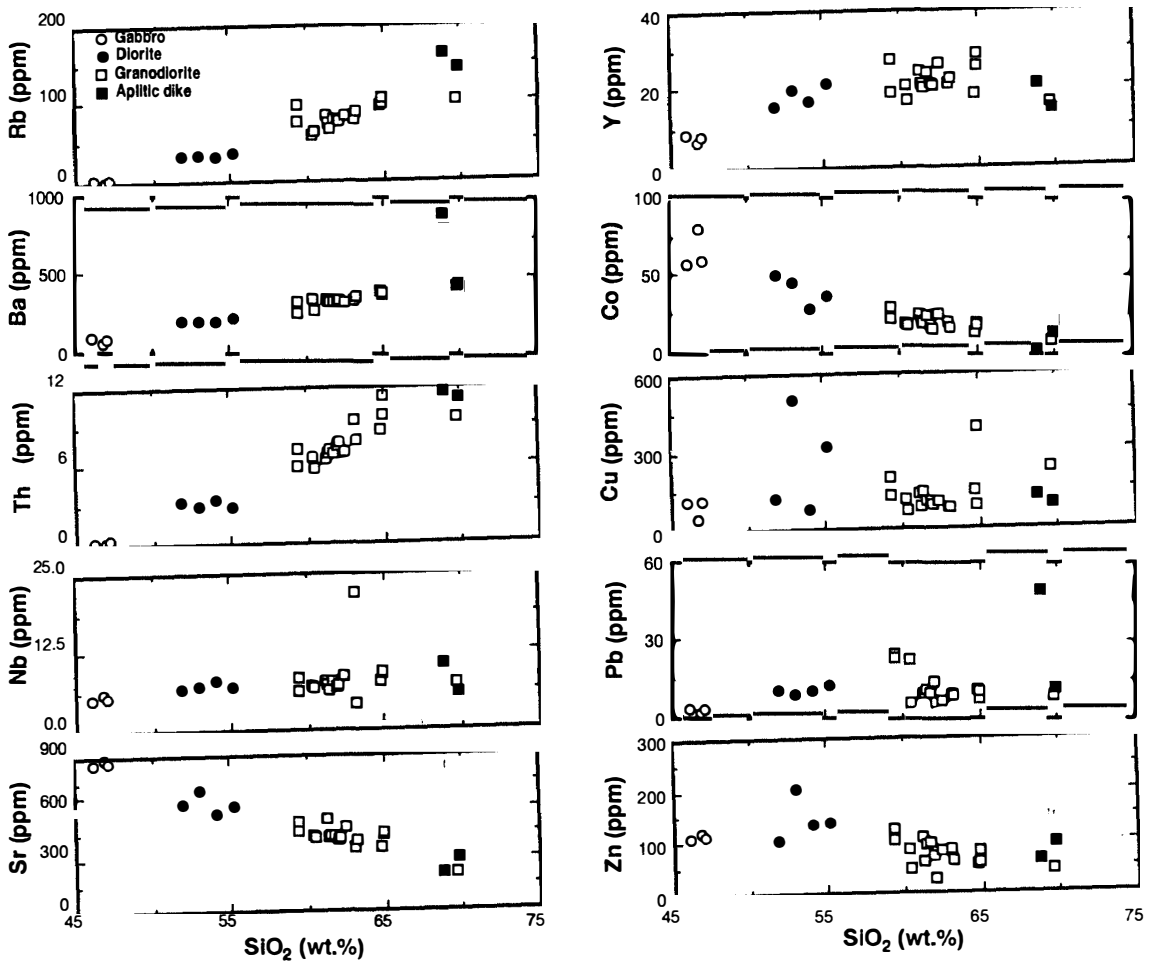

Fig. 8. Trace element variation diagrams of the granitic rocks.

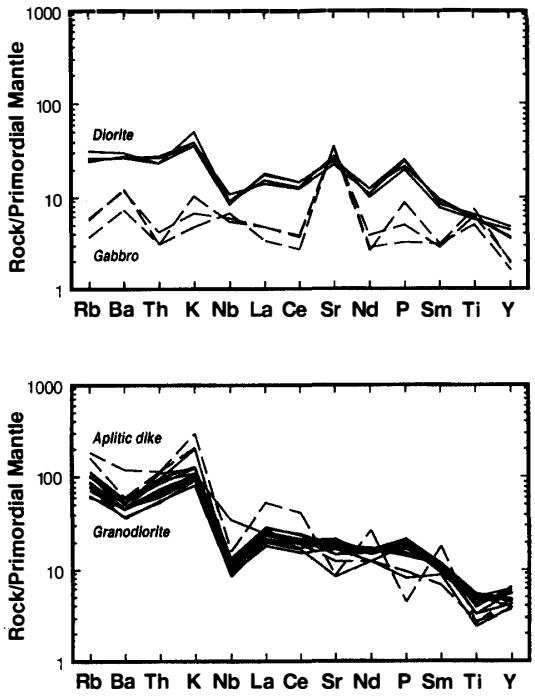

Fig. 9. Primordial mantle-normalized trace element variation diagrams (spider diagrams) of the granitic rocks. The data have been normalized to primordial mantle abundances by WOOD *et al. (1979).*

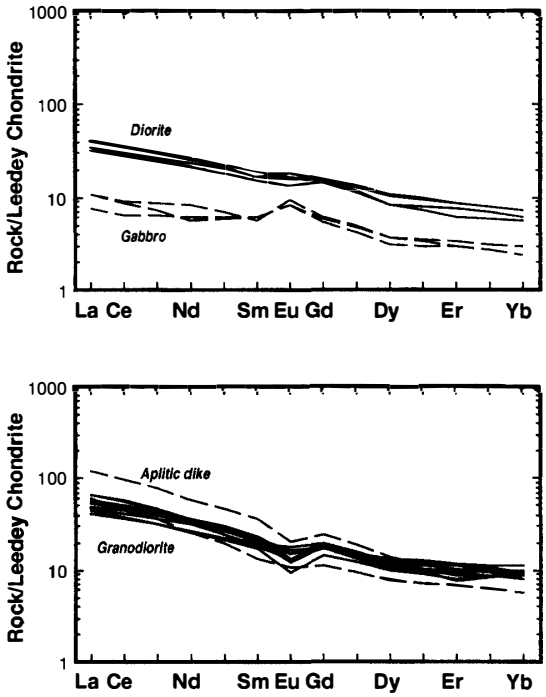

Fig. 10. Leedey chondrite-normalized rare earth element patterns of the granitic rocks. Leedey chondrite values are from MASUDA *et al. (1973).*

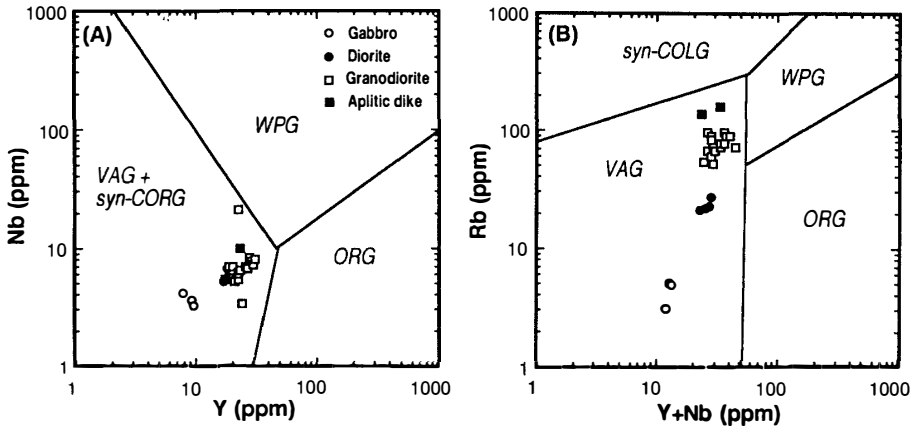

Fig. 11. Tectonic discrimination diagrams for VAG (volcanic arc granite), syn-CORG (syncollision granite), WPG (within plate granite) and ORG (ocean ridge granite) of PEARCE *et al. (1984).*

smaller than that of clacic plagioclase in a wide temperature range (MCBIRNEY, 1984). As a consequence, accumulation of calcic plagioclase would be effective in a hydrous intermediate magma at the shallow level of crust. When plagioclase sinks into a magma chamber, the intercumulus liquids remaining among the cumulus plagioclase

grains would form ferromagnesian minerals by *in situ* crystallization. It is thus considered that gabbro of the Weaver Peninsula was formed by accumulation of calcic plagioclase and *in situ* crystallization of ferromagnesian minerals near the cooling margins of a magma chamber at a shallow level of the crust.

It is notable that an accumulation process can make many subfacies which are even more mafic than the primary magma composition. Taking into account the geochemical features of gabbro as a cumulate, the primary magma of the granitic pluton in the Barton and Weaver Peninsulas is thought to have been intermediate (dioritic or quartz dioritic) in composition.

Acknowledgments

We are grateful to Dr. E.-J. PARK of Korea Basic Science Institute for the analysis of trace and rare earth elements. This work was financially supported by the Ministry of Science and Technology, Korea through KORDI (BSPN 00258-822-7).

References

BARTON, C. M. (1964): The geology of King George Island; III. The stratigraphy of King George Island. Br. Antarct. Surv., Sci. Rep., **44**, 33p.

BIRKENMAJER, K. (1983): Late Cenozoic phases of block faulting on King George Island, South Shetland Islands, West Antarctica. Bull. Acad. Pol. Sci., Terre, **30**, 21–32.

BIRKENMAJER, K., DELITALA, M. C., NEREBSKI, W., NICOLETTI, M. and PETRUCCIANI, C. (1986): Geochronology and migration of Cretaceous through Tertiary plutonic centers, South Shetland Islands (West Antarctica): Subduction and hot spot magmatism. Bull. Pol. Acad. Sci. (Earth Sci.), **34**, 243–255.

BIRKENMAJER, K., FRANCALANCI, L. and PECCERILLO, A. (1991): Petrological and geochemical constraints on the genesis of Mesozoic-Cenozoic magmatism of King George Island, South Shetland Islands, Antarctica. Antarc. Sci., **3**, 293–308.

CHUN, H. Y., CHANG, S. K. and LEE, J. I. (1994): Biostratigraphic study on the plant fossils from the Barton Peninsula and adjacent areas. J. Paleontol. Soc. Korea, **10**, 69–84.

GUTERCH, A., GRAD, M., JANIK, T. and PERCHUC, E. (1990): Tectonophysical models of the crust between the Antarctic Peninsula and the South Shetland Trench. Geological Evolution of Antarctica, ed. by M. R. A. THOMSON *et al.* Cambridge, Cambridge Univ. Press, 499–504.

HINE, R., WILLIAMS, I. S., CHAPPELL, B. W. and WHITE, A. J. R. (1978): Contrasts between I- and S-type granitoids of the Kosciusko batholith. J. Geol. Soc. Aust., **25**, 219–234.

HWANG, J., LEE, J. I. and KIM, Y. (1996): Copper mineralization of granodiorite in the Barton Peninsula, King George Island, Antarctica. J. Geol. Soc. Korea, **32** (in press).

IUGS (1973): Classification and nomenclature of plutonic rocks: recommendations. Geol. News Lett., **2**, 110–127.

KANG, P. C. and JIN, M. S. (1989): Petrology and geologic structures of the Barton Peninsula, King George Island, Antarctica. Antarctic Science: Geology and Biology, ed. by H. T. HUH *et al.* Seoul, Korea Ocean Research & Development Institute, 121–135.

KUNO, H. (1968): Differentiation of basaltic magmas. Basalts: The Poldervaart Treatise on Rocks of Basaltic Composition, 2, ed. by H. H. HESS and A. POLDERVAART. New York, Interscience, 623–688.

KUSHIRO, I. (1989): Density of magma at high pressures and melting of mantle wedge. J. Mineral. Petrol. Econ. Geol., Spec. Vol., **4**, 131–142 (in Japanese).

LEE, J. I. (1994): A study on the development of quantitative analytical program of the granitic rocks using an X-ray fluorescence. KORDI Report, BSPE 00431-671-7, 43p. (in Korean).

LEE, J. I., CHUN, H. Y. and KIM, H. (1994): Petrography of the granitic rocks distributed in the Barton and Weaver Peninsulas, King George Island. The research on natural environments and resources of Antarctica. KORDI Report, BSPN 00221-702-7, 67-97 (in Korean).

MASUDA, A., NAKAMURA, N. and TANAKA, T. (1973): Fine structures of mutually normalized rare earth patterns of chondrites. Geochim. Cosmochim. Acta, **37**, 239–248.

MCBIRNEY, A. R. (1984): Igneous Petrology. San Francisco, Freeman, Cooper & Co., 509p.

MCCULLOCH, M. T. and GAMBLE, J. A. (1991): Geochemical and geodynamical constraints on subduction zone magmatism. Earth Planet. Sci. Lett., **102**, 358–374.

NAGAO, K., OGATA, A., MIURA, Y. N. and YAMAGUCHI, K. (1996): Ar isotope analysis for K-Ar dating using two modified-VG5400 mass spectrometers - I: Isotopic dilution method. J. Mass Spectrom. Soc. Jpn., **44**, 39–61.

PANKHURST, R. J. and SMELLIE, J. L. (1983): K-Ar geochronology of the South Shetland Islands, Lesser Antarctica: Apparent lateral migration of Jurassic to Quaternary island arc volcanism. Earth Planet. Sci. Lett., **66**, 214–222.

PARK, B.-K. (1989): Potassium-Argon radiometric ages of volcanic and plutonic rocks from the Barton Peninsula, King George Island, Antarctica. J. Geol. Soc. Korea, **25**, 495–497.

PEARCE, J. A., HARRIS, N. B. W. and TINDLE, A. G. (1984): Trace element discrimination diagrams for the tectonic interpretation of granitic rocks. J. Petrol., **25**, 956–983.

SMELLIE, J. L., PANKHURST, R. J., THOMSON, M. R. A. and DAVIES, R. E. S. (1984): The geology of the South Shetland Islands: VI. Stratigraphy, geochemistry and evolution. Br. Antarct. Surv., Sci. Rep., **87**, 85p.

WATTS, D. R. (1982): Potassium-argon ages and paleomagnetic results from King George Island, South Shetland Islands. Antarctic Geoscience, ed. by C. CRADDOCK. Madison, Univ. Wisconsin Press, 255–261.

WOOD, D. A., JORON, J. L., TREUL, M., NORRY, M. and TARNEY, J. (1979): Elemental and Sr isotope variations in basic lavas from Iceland and the surrounding ocean floor. Contrib. Mineral. Petrol., **70**, 319–339.

(*Received March 18, 1996; Revised manuscript accepted August 5, 1996*)